Check for updates

Thermodynamics analysis and experiments on Ti-bearing blast furnace slag leaching enhanced by sulfuric acid roasting

Lvshan Zhou, [ID] *[b] Tongjiang Peng,*[a] Hongjuan Sun[a] and Sanyuan Wang[b]

The potential-pH diagrams of the main components of Ti-bearing blast furnace slag (air-cooled slag) at 298.15 K (25 °C) and an ion activity of 1.00 were drawn by thermodynamic calculation. Thermodynamic analysis showed that the main metal components, when the Ti-bearing blast furnace slag is roasted with concentrated sulfuric acid, could be converted to sulfate. From these analyses, it can be seen that under strong acid conditions, the major metal components could react to form sulfate, and the effective separation of Ti, Mg, and Al can be achieved from both Ca and Si. Further experiments were performed with a 5.0% dilute sulfuric acid solution used to leach a Ti-bearing blast furnace slag sample that had been calcined with concentrated sulfuric acid, at a liquid–solid ratio of 10, a reaction time of 60 min, and a reaction temperature of 338.15 K (65 °C). This led to a leaching ratio of Ti above 85.0%, leaching ratios of Mg and Al higher than 95.0%, and leaching ratios of Fe and Ca of 45.7% and 24.7%, respectively. All these values were higher than the leaching ratios of Ti-bearing blast furnace slag.

1 Introduction

The western Panxi region in China is a well-known place of origin for vanadium-bearing titanomagnetite. After beneficiation, approximately 50.0% of the titanium resources are able to enter the iron concentrate. When the blast furnace method is used to smelt the iron concentrate, the titanium resources enter the blast furnace slag, forming Ti-bearing blast furnace slag. This can afterwards be divided into water-quenched slag and air-cooled slag, according to a cooling method.[1] The applications of Ti-bearing blast furnace slag mainly include producing cement, concrete, non-fired and non-steamed bricks, functional materials, and glass-ceramics,[2,3] and also the selective extraction of valuable components such as titanium and magnesium.[4] The latter process can be mainly divided into two categories: pyrometallurgy and hydrometallurgy.[5] Besides pyrometallurgy and hydrometallurgy, there are many reports on the extraction of metals from Ti-bearing blast furnace slag with an electrochemical method, such as molten slag electrolysis, or deoxidation of a solid slag cathode.[6,7] The wet extraction process is mainly based on the sulfuric acid method,[8] hydrochloric acid method,[9] or sodium hydroxide method,[10] among other

examples. Some research achievements from these works are listed in Table 1. To obtain an air-cooled slag with good crystallinity, the valuable component leaching ratio needs to be low, by using direct acid leaching. To overcome the leaching bottleneck, a salt or acid roasting leaching process represented by ammonium sulfate[11,12] and activated roasting-alkali leaching processes[13] were reported. In other solid waste applications, the acid roasting leaching process[14] has also been effectively developed, providing a reference for the use of Ti-bearing blast furnace slag. Although the new technology has solved the problem of a low leaching ratio, there is still a lack of studies regarding leaching thermodynamic analysis, as well as theoretical studies about the transfer and reaction of the target substance. Without this, it is not possible to achieve an effective foundation for innovation and development of leaching technology.

The potential-pH (*E*-pH) diagram (Pourbaix diagram) is mainly based on thermodynamic data, and it can reflect the stable existence and transformation trend of substances in different pH systems. It can also intuitively describe several aspects that occur in the solution, like the chemical reaction, equilibrium conditions, progress direction, reaction limits, and others.[15] Weathering has an important effect on the extraction of copper, silver, and gold from copper porphyry ore. The results of this study indicated that the mineral near-surface weathering oxidation section corresponds to the oxidation area of the *E*-pH diagram, while the non-redox enrichment area corresponds to the reducing region. The predicted product is consistent with the actual mineral composition,[15] and metal surface passivation is an important means to slow or even prevent metal corrosion.

[a]Key Laboratory of Ministry of Education for Solid Waste Treatment and Resource Recycle, Institute of Mineral Materials & Application, Sichuan Engineering Lab of Nonmetallic Mineral Powder Modification & High-quality Utilization, Center of Forecasting and Analysis, School of Environment and Resource, Southwest University of Science and Technology, Mianyang 621010, Sichuan, China. E-mail: tjpeng@swust.edu.cn; kcs103201@163.com

[b]School of Chemistry and Chemical Engineering, Sichuan University of Arts and Science, Dazhou 635000, Sichuan, China

Table 1   Research achievements on recovery of valuable components from Ti-bearing blast furnace slag (in part)

No.	Leaching agent	Target component	Operating conditions	Result	Reference
1	50.0 wt% H_2SO_4	Ti	Stirring speed 400 rpm, liquid–solid weight ratio 10, reaction temperature 100 °C, reaction time 1 h	72.3% (water quenched slag) 45.0% (air-cooled slag)	8
2	20.0 wt% HCl	Ti	Stirring, liquid–solid ratio 100 mL g^{-1}, reaction temperature 100 °C, reaction time 8 h	44.0% (air-cooled slag)	9
3	2.0 mol L^{-1} NaOH	V	Ti-bearing blast furnace slag was modified with titanium slag, SiO_2 and O_2 at 1450 °C, stirring speed 500 rpm, liquid–solid ratio 3, leaching temperature 95 °C, and leaching time 90 min	91.3%	10
4	2.0 mol L^{-1} HCl	Ti	Ti-bearing blast furnace slag was modified with titanium slag, SiO_2 and O_2 at 1450 °C, stirring speed 500 rpm, liquid–solid ratio 3, leaching temperature 65 °C, and leaching time 60 min	97.8%	10
5	10.0 wt% H_2SO_4	Ti	Ti-bearing blast furnace slag was roasted with ammonium sulfate, stirring speed 450 rpm, liquid–solid ratio 5 mL g^{-1}, leaching temperature 90 °C, leaching time 3 h	94.5%	11
6	2.5 wt% H_2SO_4	Ti	Sulfuric acid curing, stirring speed 300 rpm, leaching temperature 25 °C, leaching time 3 h	85.96%	12
7	H_2O	Al	Ti-bearing blast furnace slag was roasted with NaOH, stirring, liquid–solid ratio 10 mL g^{-1}, leaching temperature 90 °C, leaching time 3 h	83.0%	13

Chandra-ambhorn et al.[16] used the E-pH diagram to speculate on the corrosion and passivation of 316 L stainless steel in a mixed solution of sodium chloride and sodium sulfate, verifying the results with lab experiments. These results showed that the E-pH diagram can better predict the corrosion of 316 L stainless steel, as well as provide better theoretical support for its corrosion resistance. Metal recovery in solid waste is an important way to realize solid waste resource utilization. Mu et al.[17] reported the pressure conditions and product distribution of leaching vanadium-containing titanium slag, according to the E-pH diagram. Ruwaida et al.[18] reported the possibility of monazite acid leaching to recover rare earth metals, based on the E-pH diagram.

Whether looking at hydrometallurgy, metal corrosion, geochemistry, or analytical chemistry, research on E-pH diagrams mostly focuses on pure metal–water systems, and there are still only a small number of studies that cover complex mineral-water systems.[19] Although the E-pH diagram is a research result under ideal conditions, it has a powerful role in the development of new industrial production processes, or even the design and preparation of new materials, while it can also provide theoretical support for practical experiments and industrial applications.

The main purpose of hydrometallurgy for Ti-bearing blast furnace slag is the separation of valuable metals.[20] Therefore, in hydrometallurgy, the key is for the target components to

dissolve as much as possible in the solution. For air-cooled slag, the high crystallization degree makes it difficult for most metals to dissolve, and theoretical research on the leaching process is relatively poor. To achieve a high-efficiency leaching, in this work, a Ti-bearing blast furnace slag was roasted using concentrated sulfuric acid, and the main focus is the chemical reaction and thermodynamics of the leaching process. Based on chemical reaction thermodynamics, E-pH diagram theory, and HSC chemistry 6.0, thermodynamic calculations were carried out, and E-pH diagrams were drawn for the sulfuric acid leaching process on Ti-bearing blast furnace slag. The main objective was to obtain a theoretical scheme for extracting valuable metals from Ti-bearing blast furnace slag, as well as provide theoretical support for the technological design of hydrometallurgy for Ti-bearing blast furnace slag.

2   Materials and methods

2.1   Materials

Titanium-bearing blast furnace slag is an air-cooled slag produced in the Panzhihua Iron and Steel Group in China. After crushing and ball milling, powder with a particle size of less than 0.150 mm is obtained. The sulfuric acid used in the experiment was analytically pure (95.0–98.0 wt%) and purchased from Chengdu Kelong Chemical Reagent Factory. Pure water produced by an ultrapure water machine (Chengdu

Ultra Pure Technology Co., Ltd., UPT-11-10T) was used in all experiments.

2.2 Experimental

According to previous work from the authors,[21] a 100 mL porcelain crucible with a lid was used, containing 10.0 g of Ti-bearing blast furnace slag sample and 15.8 g of concentrated sulfuric acid (which is 1.5 times the stoichiometric ratio of Ti, Mg, Al, and Fe in the sample). The sample was mixed well using a glass rod, and placed for 120 minutes in a 403.15 K (130 °C) tubular reactor for calcination. During the calcination process, air at 5 L min^{-1} was used to purge the generated gas, while lye and acid were used at the outlets for absorption. Roasted Ti-bearing blast furnace slag (5.0 g) was added to a 100 mL beaker to leach at different values of sulfuric acid concentrations, liquid–solid ratios, reaction times and reaction temperatures, in a constant temperature water bath (Zhengzhou Yingyu Lingke Instrument Equipment Co., Ltd., DF-101S). After the reaction, a filter was applied to obtain the filtrate and residue. The filtrate was analyzed for Ti, Mg, Al, Fe, and Ca content, the residue was washed with ultrapure water to achieve neutrality, and dried in a constant temperature drying oven at 378.15 K (105 °C), and samples were taken for chemical composition analysis. A blank group without sulfuric acid roasting was obtained during the experiment. Three parallel experiments were performed for all samples.

2.3 Analysis and characterization

The contents of Ca and Mg in the leaching solution of Ti-bearing blast furnace slag were analyzed using titration,[22] and the contents of Ti, Al, and Fe were analyzed using spectrophotometry.[23,24] The used instrument was an Evolution™ 300 UV-vis spectrophotometer, produced by Thermo Company in the United States.

Phase composition analysis was performed using an X'pert Pro X-ray diffractometer, produced by the Dutch PANalytical Company, for Ti-bearing blast furnace slag raw samples, samples after sulfuric acid roasting, and leaching residues. The test conditions were as follows: Cu target, tube voltage: 40 kV, tube current: 40 mA, transmitting slit (DS): (1/2)°, anti-scatter slit (SS): 0.04 rad, receiving slit (AAS): 5.5 mm, scanning step length: 0.02°, scan range: 3°–80°, continuous scanning.

An Axios X-ray fluorescence spectrometer with a ceramic light tube was used to analyze the chemical composition of the Ti-bearing blast furnace slag sample, with the maximum power set as 2.4 kW. Sample preparation was carried out using the fuse method.

Loss on ignition analysis was performed in a porcelain crucible with a lid that had been calcined to a constant weight. 1.00 g of Ti-bearing blast furnace slag sample (m) was added and the crucible was placed in a 1223.15 K (950 °C) muffle furnace to heat for 15–20 min. Then, the crucible was removed and placed in a desiccator to cool at room temperature, having also been weighed and calcined repeatedly until the crucible weight did not change (m_1). The loss on ignition of Ti-bearing blast furnace slag was calculated using X_{LOI} (%) $= 100(m - m_1)/m$.

2.4 E-pH diagram mapping principles

The essence of the acid leaching process is the reaction between H$^+$ ionized by the acid and the leached object, which can be expressed by the general eqn (1).[15]

$$aA + xH^+ + nE^- = bB + yH_2O \tag{1}$$
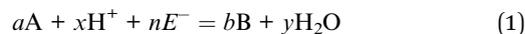
Under isothermal and isopiestic pressure conditions, and ignoring the influence of generated water, the Gibbs free energy change of the reaction can be obtained by eqn (2)–(4).

$$\Delta_r G = \Delta_r G^\theta + RT \ln[\alpha_B{}^b/(\alpha_A{}^a \cdot \alpha_{H^+}{}^x)] \tag{2}$$

$$\Delta_r G^\theta = \sum v_i \Delta_f G^\theta \text{ (product)} - \sum v_i \Delta_f G^\theta \text{ (reagent)} \tag{3}$$

$$\Delta_r G^\theta(T) = \Delta_r H^\theta(298.15 \text{ K}) - T\Delta_r S^\theta(298.15 \text{ K}) \tag{4}$$

According to the relationship between the Gibbs free energy and electric potential ($\Delta_r G = -n$FE), eqn (2) can be expressed as eqn (5).

$$n\text{FE} = -\Delta_r G^\theta - 2.303RT \lg(\alpha_B{}^b/\alpha_A{}^a) - 2.303RTx\text{pH} \tag{5}$$

When $n = 0$, the pH expression is as shown in eqn (6).

$$\text{pH} = -\Delta_r G^\theta/(2.303RTx) - \lg(\alpha_B{}^b/\alpha_A{}^a)/x \tag{6}$$

When $x = 0$, the electric potential expression is as shown in eqn (7).

$$E = -\Delta_r G^\theta/nF - 2.303RT \lg(\alpha_B{}^b/\alpha_A{}^a)/nF \tag{7}$$

When oxidation–reduction and hydrolysis–neutralization reactions coexist, the electric potential expression is as shown in eqn (8).

$$E = -\Delta_r G^\theta/nF - 2.303RT \lg(\alpha_B{}^b/\alpha_A{}^a)/nF - 2.303RTx/nF\text{pH} \tag{8}$$

3 Results and discussion

3.1 Phase and chemical composition analysis of Ti-bearing blast furnace slag (air-cooled slag)

The chemical composition analysis results of Ti-bearing blast furnace slag using the XRF analysis method are displayed in Table 2. The results indicate that the Ti-bearing blast furnace slag mainly includes Ca, Si, Ti, Al, Mg, and Fe, which account for more than 96% of the total chemical content, so the Ti-bearing blast furnace slag has a high comprehensive recycling value. The loss on ignition of the Ti-bearing blast furnace slag was only 4.75%, indicating that its structure is stable and it contains fewer components that are volatile and easy to decompose or gasify.

Fig. 1 shows the phase composition analysis of the Ti-bearing blast furnace slag (air-cooled slag), which shows that because the air-cooled slag was naturally cooled, the formed crystal phases have sharp diffraction peaks and high crystallinity. The Ti-bearing blast furnace slag mainly comprises

Table 2 The chemical composition analysis result of Ti-bearing blast furnace slag (no. BFS-1)[a]

Composition	Content/%	Composition	Content/%	Composition	Content/%
CaO	27.37	SiO_2	26.51	TiO_2	17.92
Al_2O_3	14.33	MgO	8.05	Fe_2O_3	2.59
SO_3	1.10	Na_2O	0.77	MnO	0.62
K_2O	0.58	BaO	0.07	SrO	0.04
ZrO_2	0.02	Cl	0.02	Y_2O_3	0.01
Loss on ignition	4.75				

[a] The content of main elements in high-titanium blast furnace slag is expressed in the form of oxides.
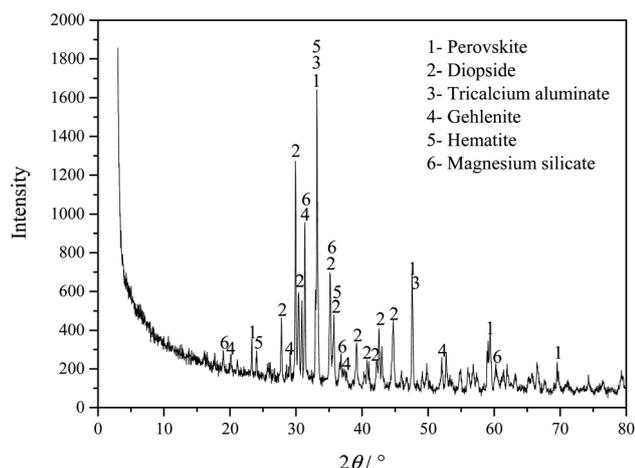
Fig. 1 XRD pattern of a Ti-bearing blast furnace slag sample.

perovskite ($CaTiO_3$, PDF#22-0153), diopside (Ca(Mg, Al))(Si, Al)$_2O_6$, (PDF#41-1370), tricalcium aluminate ($Ca_3Al_2O_6$, PDF#38-1429), gehlenite ($Ca_2Al_2SiO_7$, PDF#35-0755), hematite (Fe_2O_3, PDF# 33-0664), and magnesium silicate ($MgSiO_3$, PDF#39-0048).

3.2 Thermodynamic analysis of Ti-bearing blast furnace slag roasted with concentrated sulfuric acid

The possible reactions in the roasting process are shown in eqn (9)–(16), which take into account the roasting of Ti-bearing blast furnace slag with concentrated sulfuric acid, and the phase analysis results.

$$CaTiO_3 + 2H_2SO_4 = CaSO_4 + TiOSO_4 + 2H_2O \quad (9)$$

$$CaMgSi_2O_6 + 2H_2SO_4 = CaSO_4 + MgSO_4 + 2SiO_2 + 2H_2O \quad (10)$$

$$Ca_3Al_2O_6 + 6H_2SO_4 = 3CaSO_4 + Al_2(SO_4)_3 + 6H_2O \quad (11)$$

$$Ca_2Al_2SiO_7 + 5H_2SO_4 = 2CaSO_4 + Al_2(SO_4)_3 + SiO_2 + 5H_2O \quad (12)$$

$$MgSiO_3 + H_2SO_4 = MgSO_4 + SiO_2 + H_2O \quad (13)$$

$$Fe_2O_3 + 3H_2SO_4 = Fe_2(SO_4)_3 + 3H_2O \quad (14)$$

$$2Fe_2O_3 + 4H_2SO_4 = 4FeSO_4 + 4H_2O + O_2 \quad (15)$$

$$CaTiO_3 + H_2SO_4 = CaSO_4 + TiO_2 + H_2O \quad (16)$$
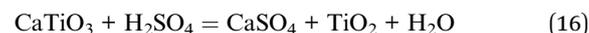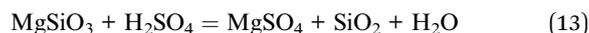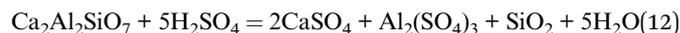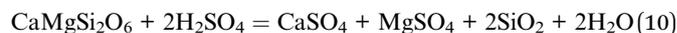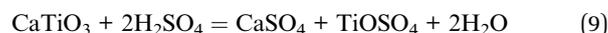
Fig. 2 shows graphs plotting the Gibbs free energy change ΔG, and equilibrium constant K for different reactions, when both Ti-bearing blast furnace slag and concentrated sulfuric acid are roasted at different temperatures. The results in Fig. 2 show that the main components in Ti-bearing blast furnace slag can spontaneously react with concentrated sulfuric acid during the roasting process. The equilibrium constants of reactions eqn (11) and (12) are very high, which indicates that the reaction proceeded very thoroughly, and the aluminum in the Ti-bearing blast furnace slag can be easily converted into soluble aluminum sulfate, which is beneficial to leaching. The Gibbs
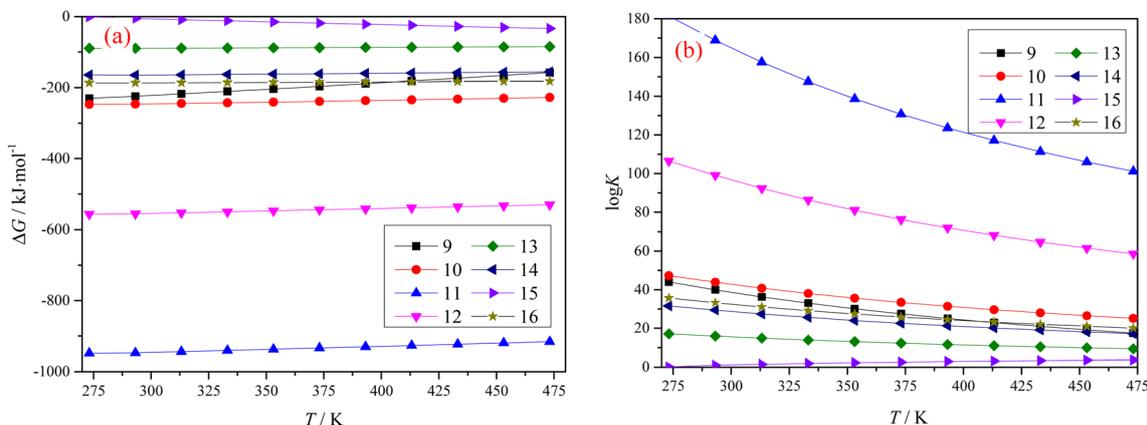

Fig. 2 Gibbs free energy change ΔG (a) and equilibrium constant K (b) of different reactions with temperature.

Table 3 Standard generated Gibbs free energies of the main substances (298.15 K, 100 kPa)[25a]

Substance	$\Delta_f G^\theta$/kJ mol^{-1}	Substance	$\Delta_f G^\theta$/kJ mol^{-1}	Substance	$\Delta_f G^\theta$/kJ mol^{-1}
$H_2(g)$	0	$H^+(aq)$	0	$H_2O(l)$	−237.1
$OH^-(aq)$	−157.3	$O_2(g)$	0	$SO_4^{2-}(aq)$	−744.5
$CaSO_4 \cdot 2H_2O(c)$	−1797.5	$CaSO_4 \cdot 0.5H_2O(c)$	−1436.8	$CaSO_4(c)$	−1309.1
$Ca(OH)_2(c)$	−897.5	$CaTiO_3(c)^*$	−1688.7	$CaMgSi_2O_6(c)^*$	−3248.8
$Ca_2Al_2SiO_7(c)^*$	−4048.5	$Ca_3Al_2O_6(c)^*$	−3649.2	$Ca^{2+}(aq)$	−553.5
$H_4SiO_4(c)$	−1333.0	$H_2SiO_3(c)$	−1092.4	$HSiO_3^-(aq)$	−1152.1
$SiO_2(c)$	−856.4	$Mg(c)$	0	$Mg^{2+}(aq)$	−454.8
$MgO(c)$	−569.3	$Mg(OH)_2(c)$	−833.7	$MgSiO_3(c)$	−1462.0
$Ti(OH)_3(c)$	−1049.8	$TiO(OH)_2(c)^*$	−1086.7	$Ti^{3+}(aq)$	−349.78
$TiO^{2+}(aq)$	−633.1	$Ti_2O_3(c)$	−1434.2	$TiOSO_4(c)^*$	−1549.9
$Fe(c)$	0	$Fe(OH)_3(c)$	−705	$Fe(OH)_2(c)$	−490.0
$Fe_2O_3(c)$	−742.2	$Fe_3O_4(c)$	−1015.4	$FeOOH(c)$	−578.0
$Fe^{3+}(aq)$	−4.7	$Fe^{2+}(aq)$	−78.9	$Al^{3+}(aq)$	−485.3
$AlO_2^-(aq)$	−830.9	$Al(OH)_3(c)$	−1306.0		

[a] c-Crystal, l-liquid, g-gas, aq-aqueous solution, *data were checked by HSC Chemistry 6.0 software.

Table 4 Reaction equilibrium equation and E-pH calculation formula of the main components of Ti-bearing blast furnace slag in the sulfuric acid system (298.15 K)

No.	Reaction	E-pH equation
a	$O_2 + 4H^+ + 4e^- = 2H_2O$	$E = 1.228 - 0.0592 \text{pH}$
b	$2H^+ + 2e^- = H_2$	$E = -0.0592 \text{pH}$
1	$CaTiO_3 + 4H^+ = Ca^{2+} + TiO^{2+} + 2H_2O$	$\text{pH} = -1.222 - 0.25 \lg([Ca^{2+}][TiO^{2+}])$
2	$CaTiO_3 + 4H^+ + SO_4^{2-} = CaSO_4 \cdot 2H_2O + TiO^{2+}$	$\text{pH} = -0.114 - 0.25 \lg([TiO^{2+}]/[SO_4^{2-}])$
3	$CaTiO_3 + 3H^+ + e^- + SO_4^{2-} + 2H_2O = CaSO_4 \cdot 2H_2O + Ti(OH)_3$	$E = -0.623 - 0.177\text{pH} - 0.0592 \lg(1/[SO_4^{2-}])$
4	$2CaTiO_3 + 6H^+ + 2SO_4^{2-} + 2e^- = 2CaSO_4 \cdot 0.5H_2O + Ti_2O_3 + 2H_2O$	$E = -0.437 - 0.178\text{pH} - 0.0296 \lg(1/[SO_4^{2-}]^2)$
5	$CaTiO_3 + 4H^+ + SO_4^{2-} = Ca^{2+} + TiOSO_4 + 2H_2O$	$\text{pH} = 6.324 - 0.25 \lg([Ca^{2+}]/[SO_4^{2-}])$
6[a]	$CaTiO_3 + 4H^+ + 2SO_4^{2-} = CaSO_4 \cdot 2H_2O + TiOSO_4$	$\text{pH} = 4.873 - 0.25 \lg(1/[SO_4^{2-}]^2)$
7	$CaTiO_3 + SO_4^{2-} + 6H^+ + e^- = CaSO_4 \cdot 2H_2O + Ti^{3+} + H_2O$	$E = -0.506 - 0.355\text{pH} - 0.0592 \lg([Ti^{3+}]/[SO_4^{2-}])$
8[a]	$CaMgSi_2O_6 + 4H^+ + 2H_2O = Ca^{2+} + Mg^{2+} + 2H_4SiO_4$	$\text{pH} = 5.919 - 0.25 \lg([Ca^{2+}][Mg^{2+}])$
9[a]	$CaMgSi_2O_6 + 4H^+ = Ca^{2+} + Mg^{2+} + 2SiO_2 + 2H_2O$	$\text{pH} = 7.155 - 0.25 \lg([Ca^{2+}][Mg^{2+}])$
10[a]	$CaMgSi_2O_6 + 4H^+ = Ca^{2+} + Mg^{2+} + 2H_2SiO_3$	$\text{pH} = 7.040 - 0.25 \lg([Ca^{2+}][Mg^{2+}])$
11[a]	$CaMgSi_2O_6 + 4H^+ + SO_4^{2-} + 4H_2O = CaSO_4 \cdot 2H_2O + Mg^{2+} + 2H_4SiO_4$	$\text{pH} = 7.043 - 0.25 \lg([Mg^{2+}]/[SO_4^{2-}])$
12[a]	$CaMgSi_2O_6 + 2H^+ + SO_4^{2-} + 4H_2O = CaSO_4 \cdot 2H_2O + Mg(OH)_2 + 2H_2SiO_3$	$\text{pH} = 7.918 - 0.5 \lg(1/[SO_4^{2-}])$
13[a]	$CaMgSi_2O_6 + 2H^+ + SO_4^{2-} + 2H_2O = CaSO_4 \cdot 2H_2O + Mg(OH)_2 + 2SiO_2$	$\text{pH} = 8.148 - 0.5 \lg(1/[SO_4^{2-}])$
14	$Ca_3Al_2O_6 + 12H^+ = 3Ca^{2+} + 2Al^{3+} + 6H_2O$	$\text{pH} = 5.905 - 0.0833 \lg([Ca^{2+}]^3[Al^{3+}]^2)$
15[a]	$Ca_3Al_2O_6 + 6H^+ = 3Ca(OH)_2 + 2Al^{3+}$	$\text{pH} = 7.790 - 0.167 \lg[Al^{3+}]^2$
16[a]	$Ca_3Al_2O_6 + 12H^+ + 3SO_4^{2-} = 3CaSO_4 \cdot 2H_2O + 2Al^{3+}$	$\text{pH} = 10.662 - 0.0833 \lg([Al^{3+}]^2/[SO_4^{2-}]^3)$
17[a]	$Ca_2Al_2SiO_7 + 4H^+ + 3H_2O = 2Ca^{2+} + 2Al(OH)_3 + H_4SiO_4$	$\text{pH} = 8.804 - 0.25 \lg[Ca^{2+}]^2$
18[a]	$Ca_2Al_2SiO_7 + 4H^+ + 2H_2O = 2Ca^{2+} + 2Al(OH)_3 + H_2SiO_3$	$\text{pH} = 8.788 - 0.25 \lg[Ca^{2+}]^2$
19	$Ca_2Al_2SiO_7 + 10H^+ = 2Ca^{2+} + 2Al^{3+} + 4H_2O + H_2SiO_3$	$\text{pH} = 1.224 - 0.1 \lg([Ca^{2+}]^2[Al^{3+}]^2)$
20	$Ca_2Al_2SiO_7 + 10H^+ + 2SO_4^{2-} + H_2O = 2CaSO_4 \cdot 2H_2O + 2Al^{3+} + H_4SiO_4$	$\text{pH} = 2.172 - 0.1 \lg([Al^{3+}]^2/[SO_4^{2-}]^2)$
21[a]	$Ca_2Al_2SiO_7 + 4H^+ + 2SO_4^{2-} + 7H_2O = 2CaSO_4 \cdot 2H_2O + 2Al(OH)_3 + H_4SiO_4$	$\text{pH} = 11.052 - 0.25 \lg(1/[SO_4^{2-}]^2)$
22	$Ca_2Al_2SiO_7 + 10H^+ + 2SO_4^{2-} = 2CaSO_4 \cdot 2H_2O + 2Al^{3+} + H_2SiO_3$	$\text{pH} = 2.111 - 0.1 \lg([Al^{3+}]^2/[SO_4^{2-}]^2)$
23	$Fe^{2+} + 2e^- = Fe$	$E = -0.409 - 0.0296 \lg[Fe^{2+}]$
24	$Fe^{3+} + e^- = Fe^{2+}$	$E = 0.769 - 0.0592 \lg[Fe^{2+}]/[Fe^{3+}]$
25	$Fe(OH)_3 + 3H^+ = Fe^{3+} + 3H_2O$	$\text{pH} = 1.14 - 0.333 \lg[Fe^{3+}]$
26	$Fe(OH)_3 + 3H^+ + e^- = Fe^{2+} + 3H_2O$	$E = 0.971 - 0.177\text{pH} - 0.0592 \lg[Fe^{2+}]$
27	$Fe(OH)_2 + 2H^+ = Fe^{2+} + 2H_2O$	$\text{pH} = 6.47 - 0.5 \lg[Fe^{2+}]$
28	$Fe(OH)_3 + H^+ + e^- = Fe(OH)_2 + H_2O$	$E = 0.208 - 0.059\text{pH}$
29	$Fe(OH)_2 + 2H^+ + 2e^- = Fe + 2H_2O$	$E = -0.026 - 0.059\text{pH}$
30	$Fe_2O_3 + 6H^+ = 2Fe^{3+} + 3H_2O$	$\text{pH} = -0.628 - 0.167 \lg[Fe^{3+}]^2$
31	$Fe_2O_3 + 6H^+ + 2e^- = 2Fe^{2+} + 3H_2O$	$E = 0.658 - 0.178\text{pH} - 0.0296 \lg[Fe^{2+}]$
32[a]	$Fe_3O_4 + 8H^+ + 2e^- = 3Fe^{2+} + 4H_2O$	$E = 1.092 - 0.237\text{pH} - 0.0296 \lg[Fe^{2+}]$
33[a]	$FeOOH + 3H^+ = Fe^{3+} + 2H_2O$	$\text{pH} = 0.131 - 0.333 \lg[Fe^{3+}]$
34[a]	$FeOOH + 3H^+ + e^- = Fe^{2+} + 2H_2O$	$E = 0.794 - 0.178\text{pH} - 0.0592 \lg[Fe^{2+}]$
35[a]	$FeOOH + H^+ + e^- = Fe(OH)_2$	$E = 0.0282 - 0.0592\text{pH}$
36[a]	$Fe_2O_3 + 2H^+ + 2e^- + H_2O = 2Fe(OH)_2$	$E = 0.0296 - 0.0592\text{pH}$

[a] The reaction Gibbs free energy was obtained using HSC Chemistry 6.0.
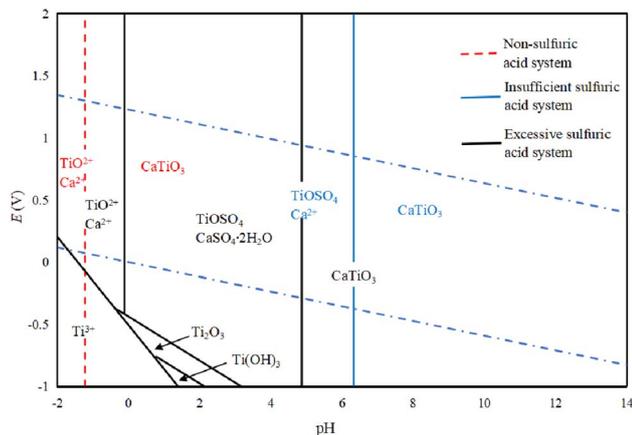
Fig. 3 The E-pH diagram of the $CaTiO_3$–H_2SO_4–H_2O system (298.15 K).

free energies of reactions eqn (13)–(15) are high, but the equilibrium constant is smaller, which means that these reactions can occur in the range of 273.15 K (0 °C) –473.15 K (200 °C), but the degree of positive reaction may not be high. Regarding reaction (16), it is possible that calcium titanate can be transformed into titanium dioxide, but titanium dioxide will decompose in hot concentrated sulfuric acid, and later transform into titanyl sulfate.[13]

3.3 E-pH diagram of the main components in Ti-bearing blast furnace slag

According to the phase and chemical composition analysis, Ti-bearing blast furnace slag mainly contains perovskite and silicate. The main components were first selected, and the drawing was carried out in light of E-pH diagram principles. Table 3 gives the standard Gibbs free energy that is required for each substance in the E-pH diagram drawing process. When drawing the E-pH diagram of the main component in the Ti-bearing blast furnace slag with a sulfuric acid solution system, the ion

concentration is used instead of the ion activity. It is supposed that each ion concentration in the system is 1 mol L^{-1}, and at 298.15 K (25 °C), both the main reaction equilibrium equation and the calculation formula of E-pH are listed in Table 4.

Fig. 3 shows the E-pH diagram of perovskite in a sulfuric acid solution system, which leads to the conclusion that $CaTiO_3$ is relatively stable in a generally aqueous solution system, while TiO^{2+} will only be generated when the pH is lower than -1.20. In a sulfuric acid solution system, $CaTiO_3$ can react with H_2SO_4 to generate a more soluble $TiOSO_4$, where the pH of TiO^{2+} is higher than the one without sulfuric acid. When the sulfuric acid amount is insufficient, calcium is present as Ca^{2+}, while in the case when the amount is sufficient, $CaSO_4 \cdot 2H_2O$ will be generated. In the low potential area, the Ti in $CaTiO_3$ can be converted to Ti^{3+}, but it is not stable and will produce $Ti(OH)_3$, Ti_2O_3, and other products.

Fig. 4 show the E-pH diagram of diopside in a sulfuric acid solution system. In the solution system, $CaMgSi_2O_6$ (diopside) can be decomposed by acid, and Si mainly exists in the form of orthosilicic or metasilicic acid. The existing forms of Mg and Ca are related to the acidic medium, and in a non-sulfuric acid system, they mainly exist in the form of Mg^{2+} and Ca^{2+}. The main reason for this is that the pH of calcium and magnesium ions that are beginning to precipitate at 298.5 K is 11.4 and 9.43, respectively. Ca^{2+} and Mg^{2+} in acidic systems can exist stably without being hydrolyzed to $Ca(OH)_2$ or $Mg(OH)_2$, while in a sulfuric acid medium, Ca mainly forms $CaSO_4 \cdot 2H_2O$, while Mg is hydrolyzed in alkaline solution to produce $Mg(OH)_2$. According to a published work, pyroxene can be decomposed under acidic conditions.[26] Regarding diopside, its acid solubility is weak, but its structure can be destroyed by ball milling, thereby increasing its decomposition rate.[27]

Fig. 5 shows an E-pH diagram of tricalcium aluminate in a sulfuric acid solution system. In an acidic system, $Ca_3Al_2O_3$ can react with acid to form soluble salts. In the case of Al^{3+}, it can be widely present in systems with a pH lower than 7.80. Because of the presence of SO_4^{2-} in the system, its existence area tends to expand for Al^{3+}, while Ca^{2+} released from other
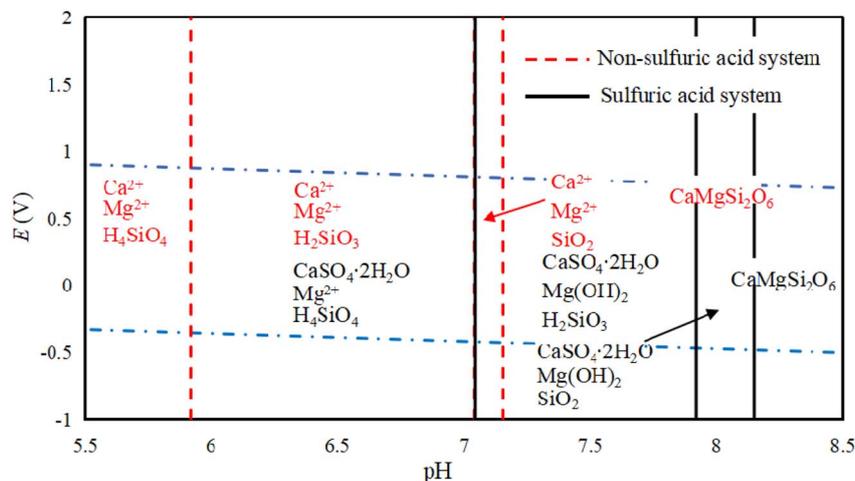

Fig. 4 The E-pH diagram of the $CaMgSi_2O_6$–H_2SO_4–H_2O system (298.15 K).
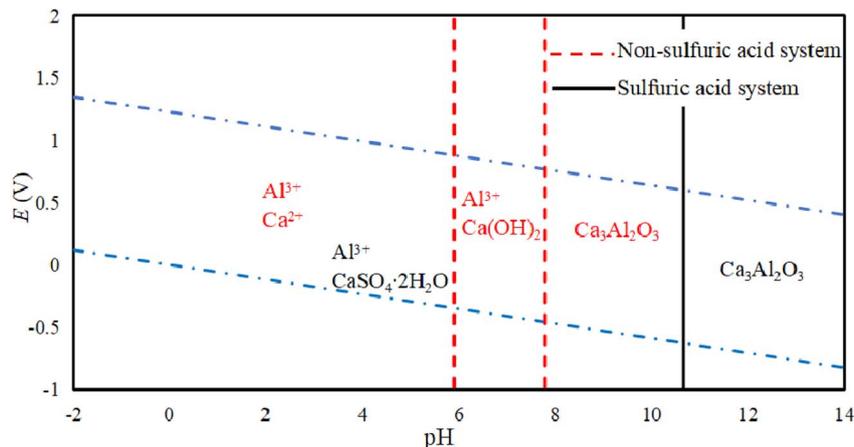
Fig. 5 The E-pH diagram of the $Ca_3Al_2O_6-H_2SO_4-H_2O$ system (298.15 K).
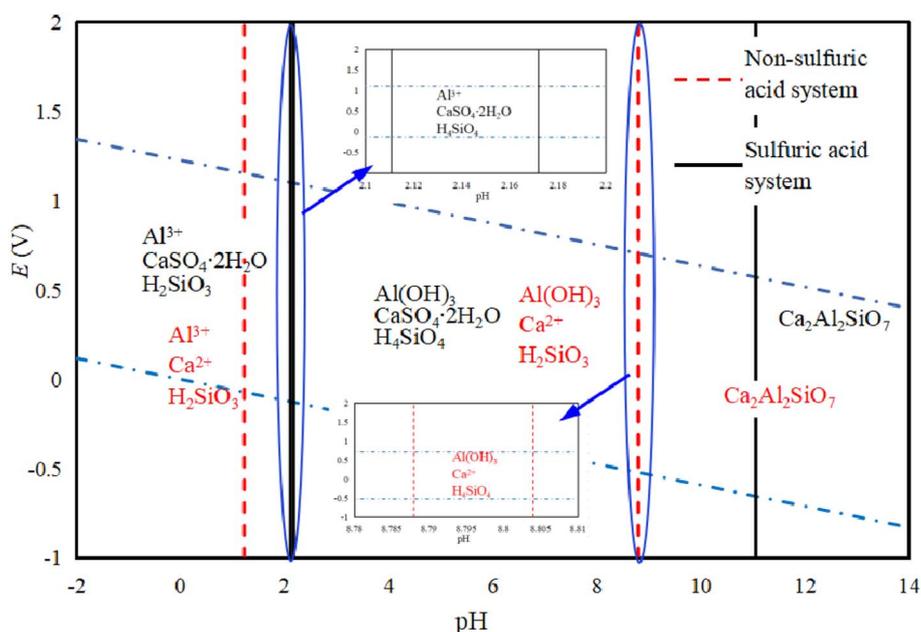
Fig. 6 The E-pH diagram of the $Ca_2Al_2SiO_7-H_2SO_4-H_2O$ system (298.15 K).

ions in the system will quickly generate calcium-containing substances with low solubility, which is consistent with conclusions of Zhao's work.[28] It is known that only when pH > 15.3 will $Al(OH)_3$ be generated, while the presence of SO_4^{2-} will increase the environmental pH requirement for $Al(OH)_3$ generation. Lapeyre *et al.*[29] found that $Ca_3Al_2O_3$ can react to form $Al(OH)_4^-$ and CaAl-OH-LDH (layered double hydroxides, LDH), and when SO_4^{2-} exists, the anions in CaAl-OH-LDH can be exchanged to form $CaAl–SO_4$-LDH. This compound is then hydrated to form $Ca_3Al_2O_6\cdot6H_2O$, although the reaction conditions are preferably alkaline.

Fig. 6 shows the E-pH diagram of yellow feldspar in the sulfuric acid solution system, illustrating that $Ca_2Al_2SiO_7$ can be converted into soluble calcium and aluminum salts under acidic conditions, where Si exists both as H_2SiO_3 or H_4SiO_4.

Under alkaline conditions, Al is converted to $Al(OH)_3$, while Ca still exists mainly as ions in the solution. When there is SO_4^{2-} in the system, Ca is converted to $CaSO_4\cdot2H_2O$, while in a system without SO_4^{2-}, Al^{3+} can exist under strong acidic conditions, where the increase in pH will promote its hydrolysis to produce $Al(OH)_3$. The experiment also showed that $Ca_2Al_2SiO_7$ can be decomposed and Al^{3+} and Ca^{2+} are released when the pH is lower than 1,[30,31] and in contrast to $Ca_3Al_2O_3$, this compound is not prone to hydration reactions.[32] There is a salt of a weak acid base containing Al and Si in the system, where the double hydrolysis reaction can promote the hydrolysis of Al^{3+}, but the conditions are not reached for $Ca(OH)_2$ precipitation in an aqueous solution system with a pH lower than 8.8.[33] In the SO_4^{2-} containing system, the conversion of Ca into
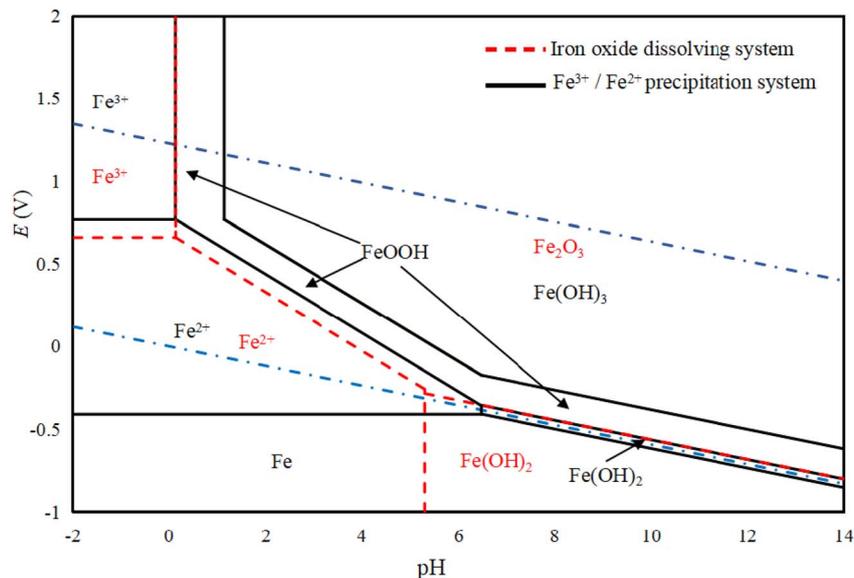
**Fig. 7** The E-pH diagram of the Fe_2O_3–H_2SO_4–H_2O system (298.15 K).

$CaSO_4 \cdot 2H_2O$ promotes the decomposition of $Ca_2Al_2SiO_7$ and increases the decomposition pH.

Based on Fig. 7, FeOOH, $Fe(OH)_3$, and Fe_2O_3 can stably exist in both the water stable region and oxygen stable region. For Fe^{2+}, its stable region is larger than that of Fe^{3+} in the water stable region, and it is possible for it to be oxidized in the aqueous solution system. When Fe_2O_3 reacts with an acid, it directly transforms to Fe^{2+} or Fe^{3+}, without undergoing the formation of FeOOH. In the case of the hydrolysis of Fe^{2+} and Fe^{3+}, FeOOH is generated first, and then oxidized to $Fe(OH)_3$, which is consistent with the actual experimental results. FeOOH can be prepared in the pH range, and it can be converted into $Fe(OH)_3$ by changing the operating conditions.[34]

3.4 Leaching of Ti-bearing blast furnace slag activated by sulfuric acid roasting

3.4.1 Effect of sulfuric acid concentration. Fig. 8 shows the effect of sulfuric acid concentration on the leaching of Ti-bearing blast furnace slag, when activated by sulfuric acid roasting. As the sulfuric acid concentration increases, the leaching ratio of the main components tends to balance out after an initial increase, while the leaching ratios of calcium and titanium are less affected by the sulfuric acid concentration. When leaching with water, the leaching ratio of titanium, aluminum, and magnesium is high, and the main reason for this is that sulfuric acid is in excess during sulfuric acid roasting, which promotes the conversion of target components to sulfate, and the excess acid dissolves in the water to provide
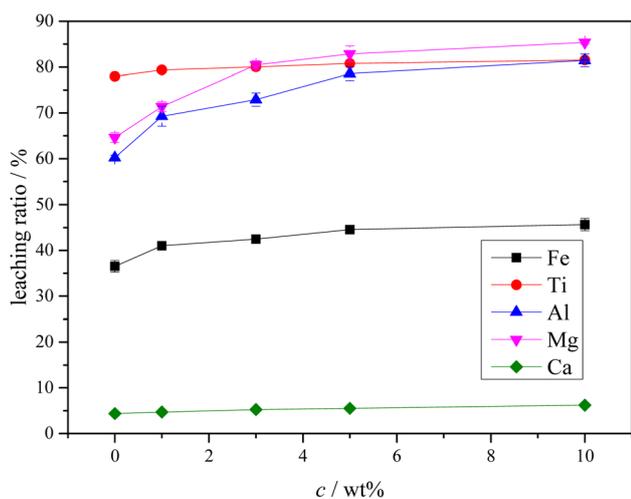

Fig. 8 Effect of sulfuric acid concentration on leaching (liquid−solid ratio: 10 mL g^{-1}, reaction temperature: 288.15 K (15 °C), reaction time: 60 min).
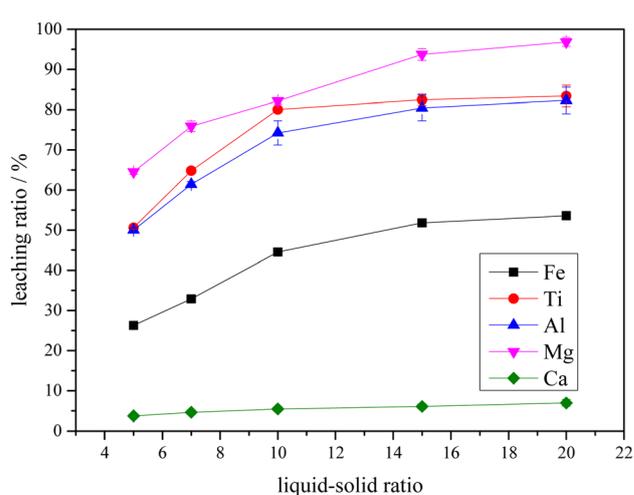

Fig. 9 Effect of liquid−solid ratio for leaching (reaction temperature: 288.15 K (15 °C), reaction time: 60 min, sulfuric acid concentration: 5.0 wt%).
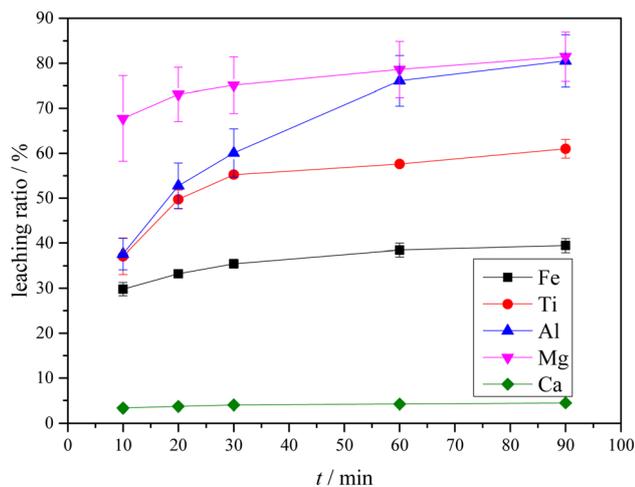
Fig. 10 Effect of reaction time on leaching (liquid–solid ratio: 10 mL g^{-1}, reaction temperature: 288.15 K (15 °C), sulfuric acid concentration: 5.0 wt%).
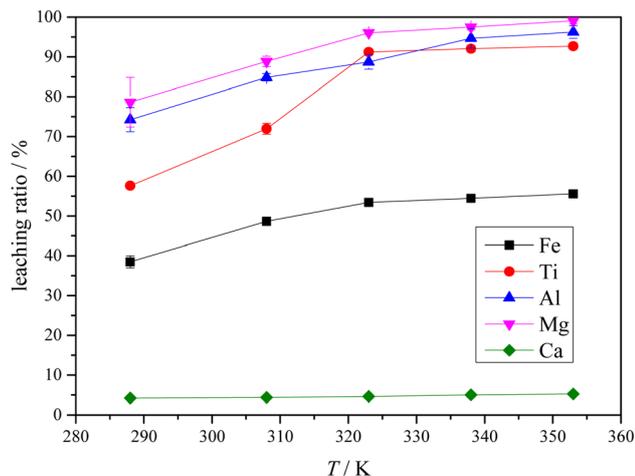

Fig. 11 Effect of reaction temperature on leaching (liquid–solid ratio: 10 mL g^{-1}, reaction time: 60 min, sulfuric acid concentration: 5.0 wt%).

acidic conditions. When a diluted sulfuric acid solution is used for leaching, the H$^+$ concentration is increased, which effectively promotes sulfate dissolution, and the components that have not been converted into sulfate dissolve in the solution system. However, excessive acid consumption will increase the economic cost and will make it difficult to use the leachate.

3.4.2 Effect of liquid–solid ratio. The result of the liquid–solid ratio for the leaching of Ti-bearing blast furnace slag activated by sulfuric acid roasting is illustrated in Fig. 9, which shows that as the liquid–solid ratio increases, the leaching ratios of titanium, aluminum, magnesium, iron, and calcium all continue to increase. In addition to calcium, other components are greatly affected by the liquid–solid ratio. The reason for this is that calcium in the solution is mainly derived from calcium sulfate dissolution during leaching. However, the solubility of calcium sulfate is small, and increasing the solution volume cannot cause a large amount of dissolution.

Although the liquid–solid ratio increase is beneficial to leaching, a large amount of leaching liquid will reduce the target component concentration, while increasing the processing difficulty of the leaching liquid. Therefore, it is more appropriate to consider a liquid–solid ratio of 10.

3.4.3 Effect of reaction time. In Fig. 10, changes in the leaching ratio of the target components of Ti-bearing blast furnace slag activated by sulfuric acid roasting for different reaction times are reflected. Fig. 10 also shows that, with prolonged reaction times, the leaching ratio of each component shows a rising trend. Although, after 60 minutes of reaction, the increasing trend significantly slows. The early leaching speed is high, since the target component concentration in the solution is low. After a period of time, the concentration increases, resulting in a decrease in mass transfer power.

3.4.4 Effect of reaction temperature. Fig. 11 shows the effect of reaction temperature on the leaching ratio of the target components of Ti-bearing blast furnace slag activated by sulfuric acid roasting. As the reaction temperature increases, the leaching ratios of iron, titanium, aluminum and magnesium all significantly increase, while the leaching ratio of calcium remained in a balanced state. Increasing the temperature has little effect on calcium leaching, although the temperature increase accelerates the irregular movement of ions in the system, promoting dissolution of the target components. When the reaction temperature exceeds 338.15 K (65 °C), the leaching ratio of each component tends to remain stable, while continuing to increase the temperature has little significance to the experiment. Therefore, the optimal reaction temperature is 338.15 K (65 °C).

3.4.5 Optimization experiment. Fig. 12 shows the different component leaching results of the Ti-bearing blast furnace slag sample after activation by sulfuric acid roasting. It also shows that the leaching ratio of Ti, Mg, or Al is approximately 45.0% for the Ti-bearing blast furnace slag roasted without sulfuric acid, and the leaching ratios of Fe and Ca are 23.1% and 1.34%, respectively. When activated by sulfuric acid roasting, the leaching ratio of Ti, Mg, or Al significantly increases. The leaching ratio of Ti was more than 85.0%, the leaching ratios of Mg and Al were higher than 95.0%, and the leaching ratios of Fe and Ca were 45.7% and 24.7%, respectively. For Ti-bearing blast furnace slag, the main valuable metals have been well extracted, and the goal of a high leaching ratio from a wet resource has been achieved.

The XRD analysis results of the Ti-bearing blast furnace slag roasted with sulfuric acid and residue of dilute sulfuric acid solution leaching are shown in Fig. 13. In Fig. 13(a), it is clear that the perovskite, pyroxene, maghemite, and tricalcium aluminate in the Ti-bearing blast furnace slag can be converted into sulfate, which is easily soluble in water, when activated by concentrated sulfuric acid roasting. Ti, Mg, Al, and Fe are converted to sulfate and dissolved in the solution, while Ca and Si are enriched in the solid phase. The experimental results show that there is still a certain amount of Fe$_2$O$_3$ (hematite) in the roasting slag (shown in Fig. 13(a)). The main reason for this is that concentrated sulfuric acid has difficulty ionizing H$^+$ in a non-water environment, which makes the acidolysis reaction
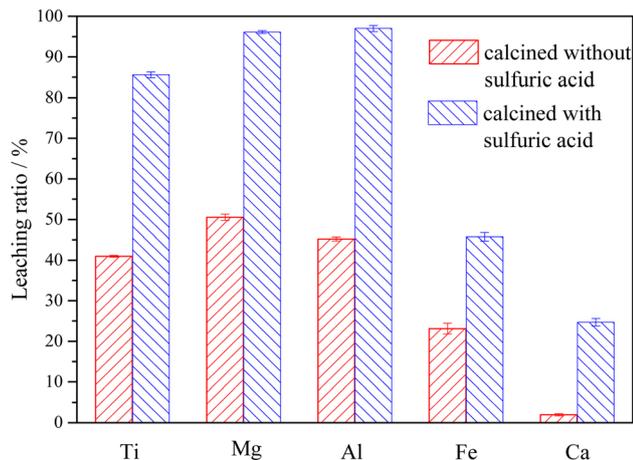
Fig. 12 Leaching ratios of Ti, Mg, Al, Fe, and Ca from Ti-bearing blast furnace slag (liquid–solid ratio: 10 mL g^{-1}, reaction temperature exceeds 338.15 K (65 °C), reaction time: 60 min, sulfuric acid concentration: 5.0 wt%).
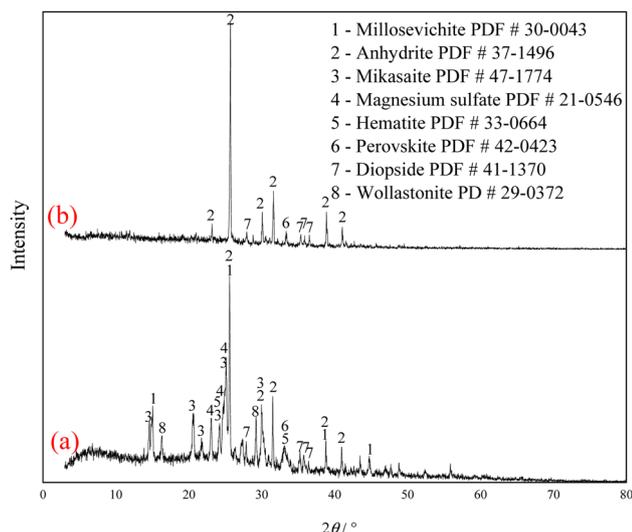

Fig. 13 XRD patterns of roasting slag (a) and remaining slag after leaching (b).

of Fe_2O_3 difficult. This achieved result is consistent with the conclusion that the equilibrium constant is small by thermodynamic analysis. There is a small amount of unreacted $CaTiO_3$ (perovskite) in the remaining slag after leaching (shown in Fig. 13(b)), and other Ti is transformed into amorphous $TiOSO_4$, which is dissolved in the sulfuric acid solution during leaching.[11] These experiments showed that the leaching solution was green, and when a small amount of potassium hexacyanoferrate(III) ($K_3[Fe(CN)_6]$) was dropped into it, a blue precipitate was generated in the solution. This phenomenon shows that there are Fe^{2+} ions in the leaching solution.

4 Conclusions

Based on the theory of chemical reaction thermodynamics and the potential-pH diagram, the reaction thermodynamics of Ti-bearing blast furnace slag activated by concentrated sulfuric acid was studied. This analysis included the design of the sulfuric acid leaching potential-pH diagram of the main components, as well as a leaching experiment of valuable components in Ti-bearing blast furnace slag roasted with sulfuric acid. The main conclusions are the following:

(1) The crystallinity degree of Ti-bearing blast furnace slag was good when it was naturally cooled in the air. The formed perovskite, diopside, tricalcium aluminate, maghemite, hematite, and magnesium silicate could spontaneously react to form sulfate in a concentrated sulfuric acid environment. In addition to the formation reaction of ferrous sulfate, the forward reaction of other chemical reactions can be promoted under heating.

(2) Based on the E-pH diagrams of $CaTiO_3$, $CaMgSi_2O_6$, $Ca_3Al_2O_3$, $Ca_2Al_2SiO_7$, and Fe_2O_3, several elements (Ti, Mg, Al, and Fe) could be converted into easily soluble sulfates, under the strong acid system, leading to the achievement of the purpose of their effective separation from Ca and Si.

(3) The Ti-bearing blast furnace slag roasted with concentrated sulfuric acid at 403.15 K (130 °C) was used for leaching. When the leaching agent was a 5% dilute sulfuric acid solution, the reaction operating parameters were: a liquid–solid ratio of 10, a reaction time of 60 min, and a reaction temperature of 338.15 K (65 °C). This led to a leaching ratio of Ti over 85.0%, leaching ratios of Mg and Al higher than 95.0%, and leaching ratios of Fe and Ca of 45.7% and 24.7%, respectively, which are higher than the leaching ratios of Ti-bearing blast furnace slag without roasting activation under the same conditions.

(4) Compared with reports in the literature,[8] the leaching ratio of titanium increases by approximately 40%, the sulfuric acid amount is reduced by approximately 45%, and the operating conditions are milder.

Author contributions

L. Zhou contributed to the literature search, study design, experimental study, data analysis, and writing—review and editing; T. Peng contributed to the design of the work and data analysis; H. Sun and S. Wang contributed to the work of writing—review and editing.

Conflicts of interest

On behalf of all authors, the corresponding author states that there is no conflict of interest.

Acknowledgements

References

1 L. Liu and S. L. Yang, *Present State and Perspectives of Complex Utilization on Panzhihua BF Slag*, Light Metals, 2007, pp. 48–50, DOI: 10.13662/j.cnki.qjs.2007.07.013.

2 L. X. He, Application of High Ti-Bearing Blast Furnace Slag in Field of Building Materials, *Adv. Mater. Res.*, 2014, **1052**, 392–395, DOI: 10.4028/www.scientific.net/AMR.1052.392.

3 K. Chen, Y. Li, X. Meng, L. Meng and Z. Guo, New integrated method to recover the TiO_2 component and prepare glass-ceramics from molten titanium-bearing blast furnace slag, *Ceram. Int.*, 2019, **45**, 24236–24243, DOI: 10.1016/j.ceramint.2019.08.134.

4 W. Zhang, L. Zhang, Y. Li and X. Li, An environmental procedure to extract titanium components and metallic iron from Ti-bearing blast furnace slag, *Green Process. Synth.*, 2015, **4**, 307–316, DOI: 10.1515/gps-2015-0031.

5 Y. Yang, J. L. Liang, H. Li, D. X. Huo and S. S. Xie, *Resource Recycling progress of Panzhihua Titanium Bearing Blast Furnace Slag*, Multipurpose Utilization of Mineral Resources, 2018, pp. 12–15, DOI: 10.3969/j.issn.1000-6532.2018.02.003.

6 Q. Zhao, N. Ye, L. Li and F. Yan, Oxalate Coprecipitation Process Synthesis of 5 V Cathode Material $LiNi_{0.5}Mn_{1.5}O_4$ and Its Performance, *Xiyou Jinshu Cailiao Yu Gongcheng*, 2010, **39**, 1715–1718, DOI: 10.1016/S1875-5372(10)60130-0.

7 X. Zou, X. Lu, W. Xiao, Z. Zhou, Q. Zhong and W. Din, Direct electrochemical extraction of Ti5Si3 from Ti/Si-containing metal oxide compounds in molten $CaCl_2$, *Shanghai Jiaotong Daxue Xuebao*, 2013, **18**, 111–117, DOI: 10.1007/s12204-013-1373-6.

8 T. Jiang, H. G. Dong, Y. F. Guo, G. H. Li and Y. B. Yang, Study on leaching Ti from Ti bearing blast furnace slag by sulphuric acid, *Miner. Process. Extr. Metall.*, 2010, **119**, 33–38, DOI: 10.1179/037195509x12585446038807.

9 F. Jia, R. Liu and M. Yang, Leaching of High-Ti-Bearing Blast-Furnace Slag Directly in Hydrochloric Acid, *Nanjing Shida Xuebao, Ziran Kexueban*, 2012, **12**, 43–49.

10 Han, J. Zhang, J. Zhang, X. Chen and L. Zhang, Extraction of vanadium and enrichment of titanium from modified Ti-bearing blast furnace slag, *Hydrometallurgy*, 2021, **201**, 105577.

11 Z. Bian, Y. L. Feng and H. R. Li, Extraction of valuable metals from Ti-bearing blast furnace slag using ammonium sulfate pressurized pyrolysis-acid leaching processes, *Trans. Nonferrous Met. Soc. China*, 2020, **30**, 2836–2847, DOI: 10.1016/s1003-6326(20)65425-5.

12 L. Wang, L. Chen, W. Liu, G. Zhang, S. Tang, H. Yue, B. Liang and D. Luo, Recovery of titanium, aluminum, magnesium and separating silicon from titanium-bearing blast furnace slag by sulfuric acid curing–leaching, *Int. J. Miner., Metall. Mater.*, 2022, **29**, 1705–1714, DOI: 10.1007/s12613-021-2293-3.

13 S. He, T. Peng and H. Sun, Titanium Recovery from Ti-Bearing Blast Furnace Slag by Alkali Calcination and Acidolysis, *JOM*, 2019, **71**, 3196–3201, DOI: 10.1007/s11837-019-03575-9.

14 J. Kim and G. Azimi, Recovery of scandium and neodymium from blast furnace slag using acid baking-water leaching, *RSC Adv.*, 2020, **10**, 31936–31946, DOI: 10.1039/d0ra05797e.

15 H. H. Huang, The Eh-pH Diagram and Its Advances, *Metals*, 2016, **6**, 23, DOI: 10.3390/met6010023.

16 S. Chandra-ambhorn, W. Wachirasiri and G. Lothongkum, *E*-pH Diagrams for 316 L Stainless Steel in Chloride Solutions Containing SO_4^{2-}, *Anti-Corros. Methods Mater.*, 2016, **63**, 431–436, DOI: 10.1108/ACMM-10-2014-1454.

17 W. Mu, T. Zhang, Z. Dou, G. LÜ and Y. Liu, φ-pH diagram of V-Ti-H_2O system during pressure acid leaching of converter slag containing vanadium and titanium, *Trans. Nonferrous Met. Soc. China*, 2011, **21**, 2078–2086, DOI: 10.1016/s1003-6326(11)60976-x.

18 N. Y. Fatin, N. M. S. Liyana, H. W. I. Wan and A. R. Ruwaida, Thermodynamic Evaluation of the Aqueous Stability of Rare Earth Elements in Sulfuric Acid Leaching of Monazite through Pourbaix Diagram, *Anti-Corros. Methods Mater.*, 2019, **19**, 1647–1656, DOI: 10.1016/j.matpr.2019.11.193.

19 Z. Cao, B. Ma, C. Wang, Y. Chen, B. Liu, P. Xing and W. Zhang, *E*-pH diagrams for the metal-water system at 150 °C: thermodynamic analysis and application for extraction and separation of target metals from saprolitic laterite, *Miner. Eng.*, 2020, **152**, 106365, DOI: 10.1016/j.mineng.2020.106365.

20 Y. Cai, N. Song, Y. Yang, L. Sun, P. Hu and J. Wang, Recent progress of efficient utilization of titanium-bearing blast furnace slag, *Int. J. Miner., Metall. Mater.*, 2022, **29**, 22–31, DOI: 10.1007/s12613-021-2323-1.

21 S. He, Study on Principle and Chemical Kinetics of Valuable Components Extraction and Separation From Panzhihua High Titanium-Blast Furnace Slag, Doctor dissertation, Southwest University of Science and Technology, China, 2020.

22 Z. Zhang, X. H. Fan and L. H. Xue, Continuous determination of calcium and magnesium in iron ore by EDTA complexometric titration, *Yejin Fenxi*, 2011, **31**, 74–78, DOI: 10.13228/j.issn.1000.

23 *GB/T 5124.4-1985, Methods for chemical analysis of cemented carbide-the peroxide photometric method for the determination of titanium content*, China Standard Press. Beijing, 1985.

24 *GB/T 5750.6-2006, Standard Inspection Method for Drinking Water-Metal Index*. China Standard Press, Beijing, 2006.

25 J. G. Speight, *Lange's Handbook of Chemistry*, 16th edn, 2005.

26 P. Semsari Parapari, M. Irannajad and A. Mehdilo, Effect of acid surface dissolution pretreatment on the selective flotation of ilmenite from olivine and pyroxene, *Int. J. Miner. Process.*, 2017, **167**, 49–60, DOI: 10.1016/j.minpro.2017.07.017.

27 Y. Xiong, C. Li, B. Liang and J. Xie, Leaching behavior of air cooled Ti-bearing blast-furnace slag in hydrochloric acid, *Chin. J. Nonferrous Met.*, 2008, **18**, 557–563, DOI: 10.19476/j.ysxb.1004.0609.2008.03.030.

28 M. Zhao, Removal and Mechanism of Inorganic Anions from Aqueous Solution by Tricalcium Aluminate, Master degree thesis, Nanchang University, 2014.

29 J. Lapeyre, H. Ma, M. Okoronkwo, G. Sant and A. Kumar, Influence of water activity on hydration of tricalcium aluminate-calcium sulfate systems, *J. Am. Ceram. Soc.*, 2020, **103**, 3851–3870, DOI: **10.1111/jace.17046**.

30 K. K. Takaaki Wajima, H. Ishimoto, O. Tamada and T. Nishiyama, The synthesis of zeolite-P, Linde Type A, and hydroxysodalite zeolites from paper sludge ash at low temperature (80 °C): optimal ash-leaching condition for zeolite synthesis, *Am. Mineral.*, 2015, **89**, 1694–1700, DOI: **10.2138/am-2004-11-1215**.

31 T. Wajima, Effects of Step-Wise Acid Leaching with HCl on Synthesis of Zeolitic Materials from Paper Sludge Ash, *Minerals*, 2020, **10**, 402, DOI: **10.3390/min10050402**.

32 G. Li, P. B. Bai, Y. M. Tian and X. C. Kong, Preparation and Properties of Gehlenite with Magnesium Slag as a raw Material, *Journal of Taiyuan University of Science and Technology*, 2013, **34**, 435–439, DOI: **10.3969/j.issn.1673-2057.2013.06.008**.

33 J. Qin, C. Yang, C. Cui, J. Huang, A. Hussain and H. Ma, Ca^{2+} and OH^- release of ceramistes containing anorthite and gehlenite prepared from waste lime mud, *J. Environ. Sci.*, 2016, **47**, 91–99, DOI: **10.1016/j.jes.2016.03.013**.

34 X. Xiong and L. X. Zhou, synthesis of iron oxyhydroxides of different crystal forms and their roles in adsorption and removal of Cr(vi) from aqueous solutions, *Acta Petrol. Mineral.*, 2008, **27**, 559–566.